Cell Reports
Article

The Calcineurin-NFAT-Angiopoietin-2 Signaling Axis in Lung Endothelium Is Critical for the Establishment of Lung Metastases

Takashi Minami,[1,*] Shuying Jiang,[2] Keri Schadler,[3] Jun-ichi Suehiro,[1] Tsuyoshi Osawa,[1] Yuichi Oike,[4] Mai Miura,[1] Makoto Naito,[2] Tatsuhiko Kodama,[5] and Sandra Ryeom[3,*]
[1]Division of Vascular Biology, RCAST, the University of Tokyo, Tokyo 153-8904, Japan
[2]Department of Cellular Function, Niigata University, Niigata 950-2181, Japan
[3]Department of Cancer Biology, Abramson Family Cancer Research Institute, University of Pennsylvania School of Medicine, Philadelphia, PA 19104, USA
[4]Department of Molecular Genetics, Kumamoto University, Kumamoto 860-8555, Japan
[5]Systems Biology, RCAST, the University of Tokyo, Tokyo 153-8904, Japan
*Correspondence: minami@med.rcast.u-tokyo.ac.jp (T.M.), sryeom@upenn.edu (S.R.)
http://dx.doi.org/10.1016/j.celrep.2013.07.021

SUMMARY

The premetastatic niche is a predetermined site of metastases, awaiting the influx of tumor cells. However, the regulation of the angiogenic switch at these sites has not been examined. Here, we demonstrate that the calcineurin and nuclear factor of activated T cells (NFAT) pathway is activated specifically in lung endothelium prior to the detection of tumor cells that preferentially metastasize to the lung. Upregulation of the calcineurin pathway via deletion of its endogenous inhibitor *Dscr1* leads to a significant increase in lung metastases due to increased expression of a newly identified NFAT target, Angiopoietin-2 (ANG2). Increased VEGF levels specifically in the lung, and not other organ microenvironments, trigger a threshold of calcineurin-NFAT signaling that transactivates *Ang2* in lung endothelium. Further, we demonstrate that overexpression of DSCR1 or the ANG2 receptor, soluble TIE2, prevents the activation of lung endothelium, inhibiting lung metastases in our mouse models. Our studies provide insights into mechanisms underlying angiogenesis in the premetastatic niche and offer targets for lung metastases.

INTRODUCTION

Metastasis is a multistep process that requires tumor cells to acquire properties that allow them to escape from the primary tumor site, travel to a distant site, seed, and form tumors. Previous studies have described the formation of a "premetastatic niche" prior to the arrival of tumor cells marked by VEGFR1$^+$ bone-marrow-derived endothelial progenitor cells or CD11b$^+$ myeloid cells, depending on the tumor model utilized (Erler et al., 2009; Kaplan et al., 2005). The development of the premetastatic niche is regulated in part by soluble factors produced by the primary tumor to communicate with cells at the future site of metastasis. The formation of micro- and macro-metastases at later stages of disease are thought to involve tumor cell recruitment of endothelial progenitor cells (De Palma et al., 2003) as well as TIE2$^+$ monocytes (De Palma et al., 2005; Welford et al., 2011) to create a proangiogenic environment with high levels of vascular endothelial growth factor (VEGF) and other proangiogenic factors, which trigger the angiogenic switch (Bergers and Hanahan, 2008; Saharinen et al., 2011). However, little is known about the role of local endothelial cell activation at the premetastatic niche or during the early stages of micrometastases formation.

We and others have previously demonstrated that a key intracellular mediator of VEGF signaling in endothelial cells is the calcineurin and nuclear factor of activated T cells (NFAT) pathway (Hesser et al., 2004; Minami et al., 2004). VEGF activation of VEGFR2 on endothelial cells leads to increased intracellular calcium and activation of the calcium regulated Ser/Thr phosphatase calcineurin. Calcineurin dephosphorylates the NFAT family of transcription factors permitting their nuclear entry and transactivation of proangiogenic genes followed by induction of its endogenous inhibitor, the Down syndrome candidate region 1 (*Dscr1*) gene (Minami et al., 2004, 2006). Upregulation of DSCR1 creates a negative feedback loop in which DSCR1 inhibits calcineurin activity by direct interaction, thus attenuating NFAT nuclear import and transactivation of its targets. To maintain vascular homeostasis under physiologic conditions, this feedback loop works to minimize endothelial cell activation in the presence of VEGF. However, during tumor progression with pathologically high levels of VEGF produced as a consequence of increasing tumor mass, calcineurin-NFAT is constitutively active as endogenous DSCR1 levels are no longer

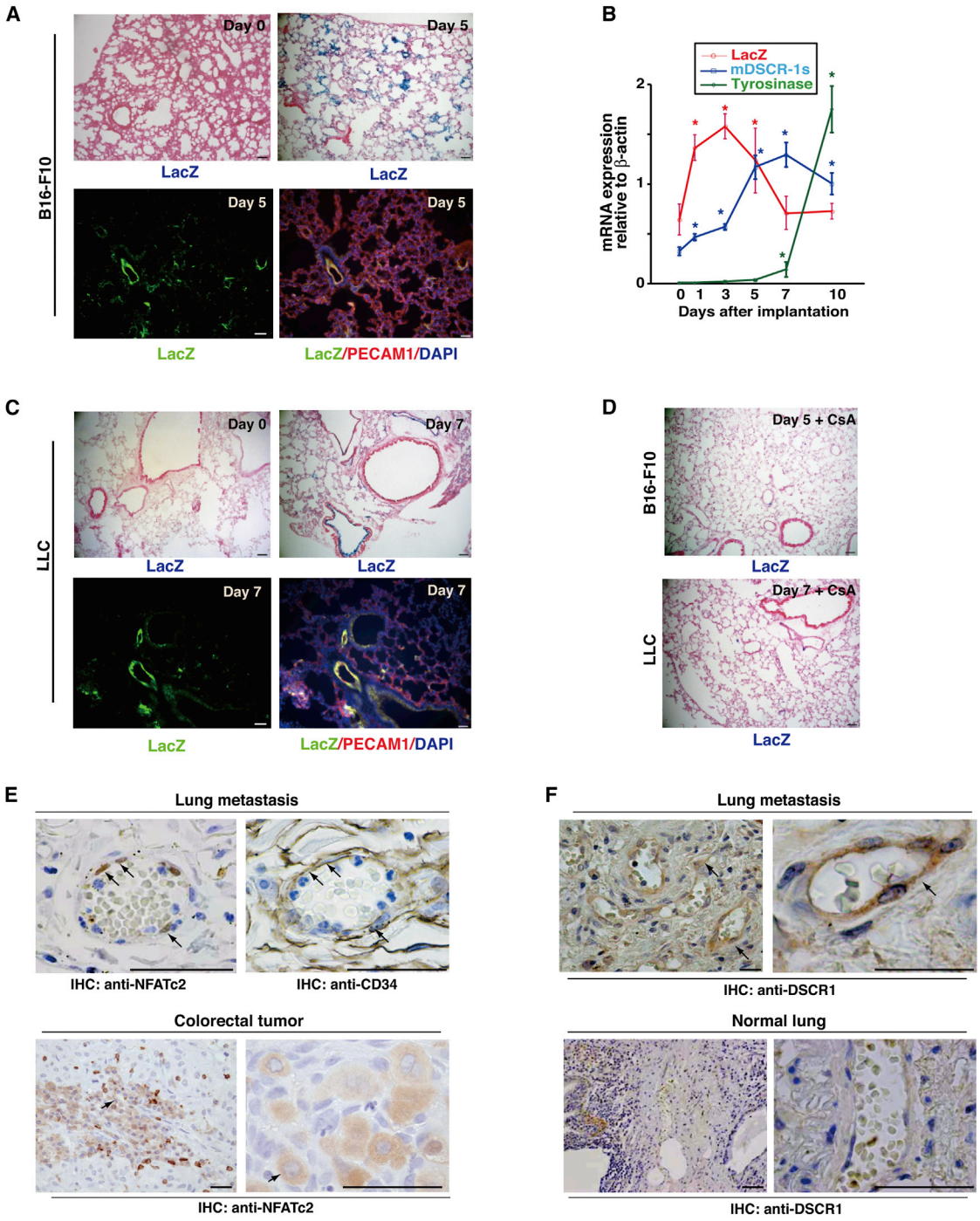

Figure 1. Calcineurin-NFAT Signaling Is Activated in Metastatic Lung Vasculature Endothelium

(A) Representative images of lung sections harvested from *Dscr1-lacZ-hprt* mice 5 days after inoculation with B16-F10 (i.v.) and immunostained with LacZ (blue or green), anti-PECAM1 (red), and DAPI. n = 6; the scale bar represents 50 μm.

(B) qPCR analysis of melanoma-specific *tyrosinase*, *lacZ* regulated by the *Dscr1* promoter, and endogenous *Dscr1* mRNA in the lungs of mice after B16-F10 tail vein injection at the indicated days. Data are presented as mean ± SEM relative to β-actin mRNA in triplicate; n = 5. *$p < 0.05$ compared to day 0 in each target gene.

(C) Representative images of lungs from *Dscr1-lacZ-hprt* mice 7 days after LLC inoculation in the flank and immunostained with LacZ (blue or green), anti-PECAM1 (red), and DAPI. n = 6; the scale bar represents 50 μm.

(D) Representative images of lungs harvested from *Dscr1-lacZ-hprt* mice with B16-F10 tumors or LLC flank tumors and treated daily with cyclosporin A (CsA) i.p. for 5 or 7 days, respectively. Lungs were sectioned and stained for LacZ. n = 6; scale bar, 50 μm.

(legend continued on next page)

sufficient to inhibit calcineurin activity. Deregulation of this pathway by either loss of *Dscr1* or trisomic expression of *Dscr1* inhibits endothelial cell activation and ultimately tumor angiogenesis during primary tumor growth by two different mechanisms (Baek et al., 2009; Ryeom et al., 2008). The role of calcineurin pathway activation in the vasculature of metastatic lesions has not yet been examined.

In the present study, we examined endothelial cell activation in early metastatic lesions and show that the calcineurin-NFAT-DSCR1 signaling axis is activated in the vasculature at these sites. Attenuation of this pathway by genetic manipulation of DSCR1 overexpression in transgenic mouse models shows inhibition of lung metastases, whereas *Dscr1* deletion and constitutively activated calcineurin accelerates the formation of lung metastases. In the metastatic lung microenvironment, we identified high levels of VEGF specifically in the lungs leading to activation of lung endothelium as indicated by high levels of VEGF receptor 2 (VEGFR2) phosphorylation and calcineurin-NFAT-mediated Angiopoietin-2 (ANG2) induction. Immunohistochemical analyses of lung metastases resected from patients with primary colorectal tumors confirmed activation of NFAT and increased expression of ANG2 specifically in the endothelium of lung metastases and not in primary colorectal tumors. Further, adenoviral-mediated delivery of soluble TIE2 to sequester ANG2 was sufficient to reverse of the formation of lung metastases in *Dscr1*-null mice. Collectively, our data provide insights into endothelial cell activation in early metastatic lesions in the lungs and point to DSCR1 and soluble TIE2 (sTIE2) as potential therapeutic targets in lung metastases.

RESULTS

Calcineurin Signaling Is Activated in the Vasculature of the Premetastatic Niche in the Lung

To examine whether calcineurin was activated in early metastatic lesions, we utilized *Dscr1-LacZ* mice in which *LacZ* was targeted into the *hprt* locus and controlled by *Dscr1*'s native promoter, allowing *Lac*Z upregulation to serve as a surrogate for calcineurin-NFAT activity. Using a lung colonization assay in these mice, we found significant LacZ expression in the lung 5 days after tail vein injection of B16-F10 melanoma cells (Figures 1A and S1A) but no expression in the liver or kidney (Figure S1B). Coimmunofluorescence of lung sections with anti-LacZ and anti-PECAM1 confirmed increased DSCR1 expression specifically in the lung endothelium as early as 5 days after melanoma cell injection (Figure 1A). To assess the arrival of tumor cells in the lungs, we quantified *tyrosinase* messenger RNA (mRNA) as a marker of melanoma cells (Figure 1B). *LacZ* mRNA as an indication of DSCR1 transcription was significantly upregulated 1 day after tumor cell injection, while *tyrosinase* mRNA expression only increased 7 days after B16-F10 inoculation. Endogenous *Dscr1* mRNA expression increased 3–5 days after tumor cell injection validating calcineurin-NFAT activation in the lung prior to detection of tumor cells (Figure 1B). To confirm these data, we utilized two other metastatic tumor models. Lewis lung carcinoma (LLC) cells injected into the flank will spontaneously metastasize to the lung and renal cell carcinoma (Renca) cells injected under the kidney capsule also metastasize to the lung. Upregulation of LacZ specifically in the lung endothelium after tumor cell inoculation was also observed in these models (Figures 1C, S1C, and S1D), with LacZ expression abrogated upon treatment with the calcineurin-specific inhibitor cyclosporin A (CsA) in both the B16-F10 and LLC tumor models (Figure 1D).

To determine whether calcineurin activation was observed in patients with metastatic disease, we examined NFAT subcellular localization by immunohistochemistry in metastatic lung lesions and found significant nuclear localization of NFATc2 in tumor endothelial cells that were labeled by CD34 staining of serial sections (Figure 1E). In contrast, NFATc2 was localized to the cytosol in endothelium and alveolar epithelium of adjacent normal lung sections (Figure S1E). DSCR1 expression was also upregulated in metastatic tumor endothelium (Figure 1F) as compared to normal lung endothelium. Examination of metastatic lesions from 20 different patients confirmed these observations (Table S1), and sections from each patient were quantified for NFAT nuclear localization (Figure S1F). Collectively, these findings imply calcineurin-NFAT activation specifically in the vasculature of metastatic lung lesions.

Loss of DSCR1 and Upregulated Calcineurin-NFAT Signaling Leads to Increased Lung Metastases

The relationship between primary tumor size and the extent of metastatic disease is not well understood. We have previously shown that primary tumor growth is significantly inhibited in *Dscr1* null mice due to suppression of tumor angiogenesis (Ryeom et al., 2008). Here, we examined the incidence of lung colonization in *Dscr1*$^{-/-}$ mice after B16-F10 injection. Ten days after intravenous (i.v.) tumor cell inoculation, there was a significant increase in gross lung lesions and decreased survival of *Dscr1*$^{-/-}$ mice versus wild-type (WT) controls (Figures 2A and 2B). Next, we utilized 3LLC tumor cells that spontaneously metastasize to the lung after subcutaneous flank injection. As expected, primary 3LLC tumor growth was significantly smaller in *Dscr1*$^{-/-}$ mice. However, macroscopic metastatic lesions were clearly visible in the lungs of *Dscr1*$^{-/-}$ mice as compared to WT controls (Figure 2C). Similarly, orthotopic injection of Renca cells into the kidney capsule and LLC footpad injection also confirmed a dramatic increase in lung metastases in mice lacking *Dscr1* (Figures 2D, 2E, S2A, and S2B). Collectively, our data using multiple tumor cell lines and models of metastases illustrate that metastases to the lung does not correlate with

(E) Representative images of sections from lung metastases (upper row) or primary colon tumors (lower row) resected from patients and immunostained with anti-NFATc2. Serial sections from lung metastases were immunostained with the endothelial marker anti-CD34 on the right. The scale bar represents 50 μm. Arrow indicates nuclear localized NFATc2 in endothelium. Sections from n = 20 patients were examined.

(F) Representative images of sections from lung metastases or adjacent normal lung tissue resected from patients and immunostained with anti-DSCR1. The scale bar represents 50 μm. Arrow indicates DSCR1 expression. Sections from n = 20 patients were examined.

See also Figure S1 and Tables S1, S3, and S4.

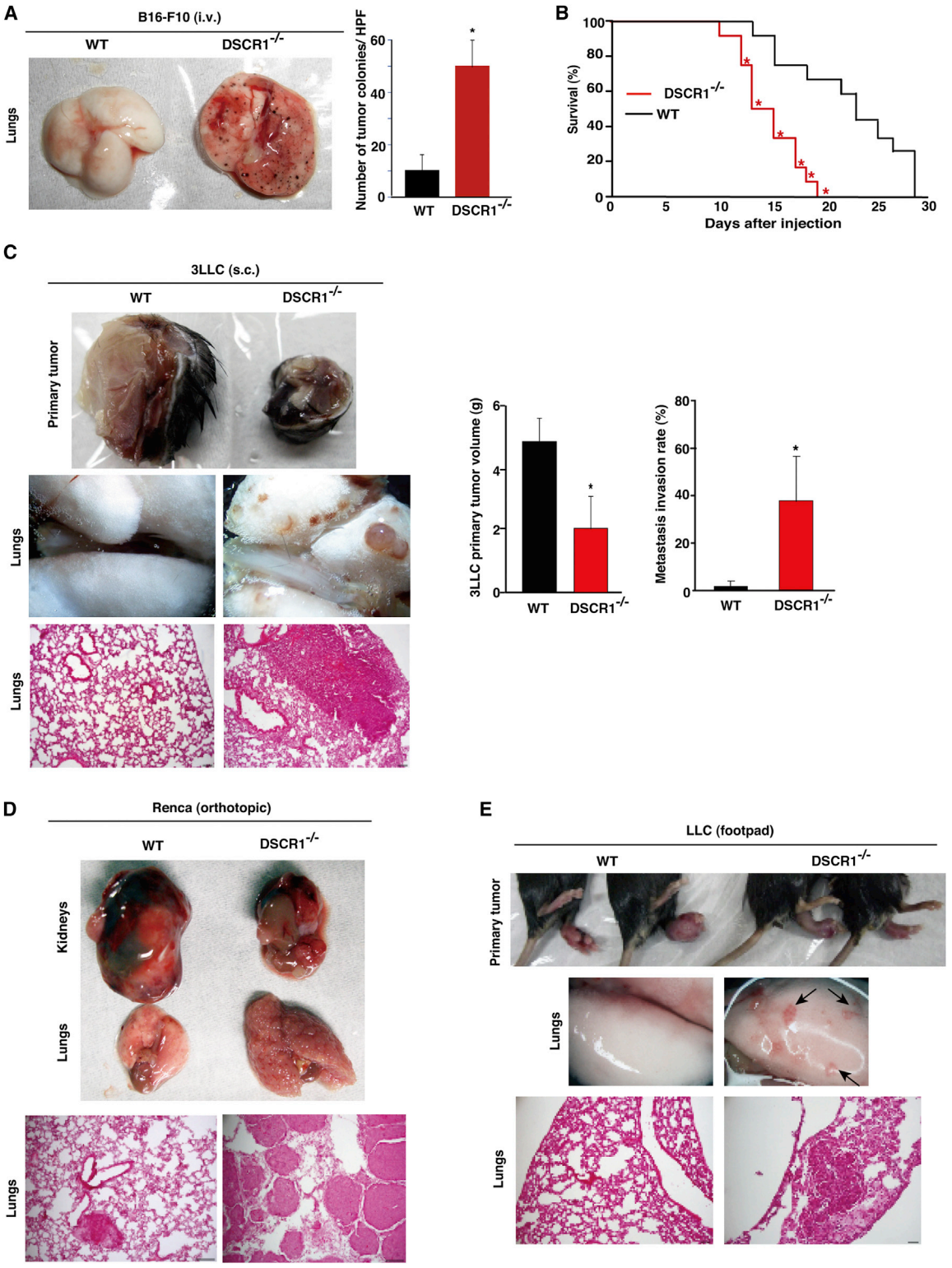

Figure 2. Deregulation of Calcineurin-NFAT Signaling by Loss of its Endogenous Inhibitor, *Dscr1*, Leads to Increased Metastases Even with Decreased Primary Tumor Growth

(A) Representative images of lungs harvested 10 days after WT or *Dscr1*$^{-/-}$ mice were injected with B16-F10 (i.v.) cells. n = 10. Quantification of the number of tumor colonies per high-powered field (hpf) is on the right.

(B) Kaplan-Meyer survival curves of B16-F10-bearing WT or *Dscr1*$^{-/-}$ mice (n = 12). *p < 0.01 compared to WT in each day.

(legend continued on next page)

primary tumor size and that upregulation of calcineurin signaling due to loss of *Dscr1* promotes metastatic progression.

Our prior studies demonstrated that calcineurin hyperactivation in the vasculature during primary tumor growth suppressed angiogenesis by promoting endothelial cell apoptosis due to precocious NFAT-dependent transactivation of Fas ligand (Ryeom et al., 2008). Thus, we examined endothelial cell apoptosis in the lungs of *Dscr1*$^{-/-}$ mice after B16-F10 inoculation by staining for TUNEL^{+}PECAM^{+} cells. In comparison to mice injected with the bacterial toxin lipopolysaccharide (LPS), which triggers widespread endothelial cell death in the lungs (Minami et al., 2009), *Dscr1*$^{-/-}$ mice injected with tumor cells showed no TUNEL-positive lung endothelial cells (Figure S2C). To investigate the mechanism by which calcineurin hyperactivation promotes lung metastases, we performed a complementary DNA (cDNA) microarray on primary lung endothelial cells isolated from WT and *Dscr1*$^{-/-}$ mice treated with VEGF to identify differentially expressed genes. A heatmap generated from this data did not show Fas ligand upregulation, but it did identify a number of genes that were highly expressed in *Dscr1*$^{-/-}$ lung endothelial cells (Figure 3A). While the expected NFAT-dependent inflammatory and proangiogenic genes were upregulated, we found that *Ang2* levels were also significantly increased in primary *Dscr1*$^{-/-}$ mouse lung endothelial cells (Figure 3A) and in human lung endothelial cells after *Dscr1* knockdown (Figure 3B). Quantitative PCR (qPCR) analyses demonstrated decreased *Dscr1* mRNA in human lung endothelium after DSCR1 knockdown using si-*Dscr1* constructs and confirmed increased *Ang2* mRNA expression in these cells (Figure 3C). Microarray analysis of human endothelial cells infected with either adenoviral *Dscr1* or a control vector further confirmed the calcineurin-NFAT dependence of *Ang2* as it was found to be the most downregulated gene in the presence of DSCR1 overexpression after VEGF treatment (Figure S3A). Moreover, significantly decreased *Ang2* mRNA expression in VEGF-treated lung endothelial cells with DSCR1 overexpression was detected by qPCR, confirming its regulation by calcineurin-NFAT signaling (Figure S3B).

ANG2 is related to ANG1, a family of endothelial-specific cytokines whose receptors are the TIE1 and TIE2 receptor tyrosine kinases. ANG2 expression is tightly regulated both at the transcriptional and posttranscriptional levels and is produced predominantly by activated endothelium counteracting blood vessel stability mediated by ANG1 (Eklund and Saharinen, 2013). Although GATA2 and Ets1 have been shown to regulate the ANG2 promoter (Hegen et al., 2004; Simon et al., 2008), a role for the NFAT family of transcription factors in ANG2 expression has not been previously investigated, although multiple NFAT binding sites were identified in introns 1 and 2 of the *Ang2* enhancer region (Figure 3D). An NFATc1 chromatin immunoprecipitation (ChIP) of human lung endothelial cells showed that NFATc1 specifically binds introns 1 and 2 in the *Ang2* enhancer region after VEGF treatment (Figures 3E and S4A), with expression of NFATc1 also activating an *Ang2* reporter containing either intron 1 or intron 2 or both (Figure 3F). VEGF treatment of lung endothelial cells transfected with the *Ang2* reporter demonstrated activation of reporter constructs when intron 1 or 2 were present which were inhibited by CsA (Figure S4B), confirming the calcineurin-NFAT-dependent regulation of *Ang2* expression in endothelial cells after VEGF treatment.

VEGF and ANG2 Expression in the Vasculature of Lung Metastases

While *Ang2* mRNA levels in the lungs of B16-F10 tumor-bearing WT and *Dscr1*$^{-/-}$ mice were initially similar, its expression was dramatically upregulated in *Dscr1*$^{-/-}$ lungs beginning 6 days after tumor cell injection (Figure 4A). Presumably, the lack of calcineurin inhibition by DSCR1 prevents *Ang2* expression in the lungs from plateauing, as observed in WT mice, but instead leads to increased calcineurin-NFAT activity and notably higher levels of *Ang2* message. Immunofluorescence analysis indicates endothelial expression of ANG2 by colocalization with PECAM1 (Figure 4B). ANG2 levels were significantly increased in the plasma of tumor-bearing mice and were also upregulated specifically in the lung, but not in the heart (Figure 4C). The lack of increased ANG2 levels in primary tumors further suggests an ANG2 specific role in early metastatic lesions (Figure 4D). To determine whether ANG2 expression in lung metastases is reflected in patients, we screened for ANG2 expression in lung metastases, primary lung adenocarcinoma, and squamous cell carcinomas by immunohistochemistry. Significant ANG2 expression was detected in metastatic lung endothelium as compared to the vasculature of primary lung tumors or in normal lung endothelium (Figures 4E and S5).

Upregulated ANG2 levels antagonize ANG1-TIE2 interactions, causing vessel regression that leads to hypoxia and a subsequent increase in VEGF production (Holash et al., 1999). Thus, increased ANG2 expression in the lungs of *Dscr1*$^{-/-}$ mice after tumor cell inoculation would predict that VEGF levels would be higher in the lungs. To test the interplay of ANG2 and VEGF in early metastatic lesions in the lung, we examined both VEGF levels and VEGFR2 activation during tumor growth. VEGF was appreciably upregulated in LLC tumor-bearing *Dscr1*$^{-/-}$ mice both in the plasma and the lungs, but not in the kidney or liver, demonstrating the specificity of increased lung VEGF (Figure 5A). However, as expected, a comparison of VEGF expression in the lungs versus flank tumors demonstrated higher VEGF levels in

(C) Images of tumors or lungs harvested from WT or *Dscr1*$^{-/-}$ mice 20 days after subcutaneous (s.c.) inoculation with 3LLC cells. Representative H&E staining of lung sections are shown on the bottom. The scale bar represents 50 μm. Middle bar graph: primary tumor volumes are shown (graph on left); *$p < 0.05$ compared to WT; n = 6. The metastases invasion rate (graph on right) was quantified as the ratio of metastatic area versus normal lung area. *$p < 0.001$ compared to WT; n = 6.

(D) Representative images of tumors or lungs harvested from WT or *Dscr1*$^{-/-}$ mice 30 days after orthotopic implantation of Renca cells under the kidney capsule. Representative H&E staining of lung sections are shown on the bottom. The scale bar represents 50 μm. Data are representative of six independent experiments.

(E) Representative images of tumors or lungs harvested from WT or *Dscr1*$^{-/-}$ mice 14 days after footpad implantation of LLC cells. Representative H&E stains from lung tissue sections are shown on the bottom. The scale bar represents 50 μm. Arrows indicate metastatic lesions. Data are representative of ten independent experiments.

See also Figure S2.

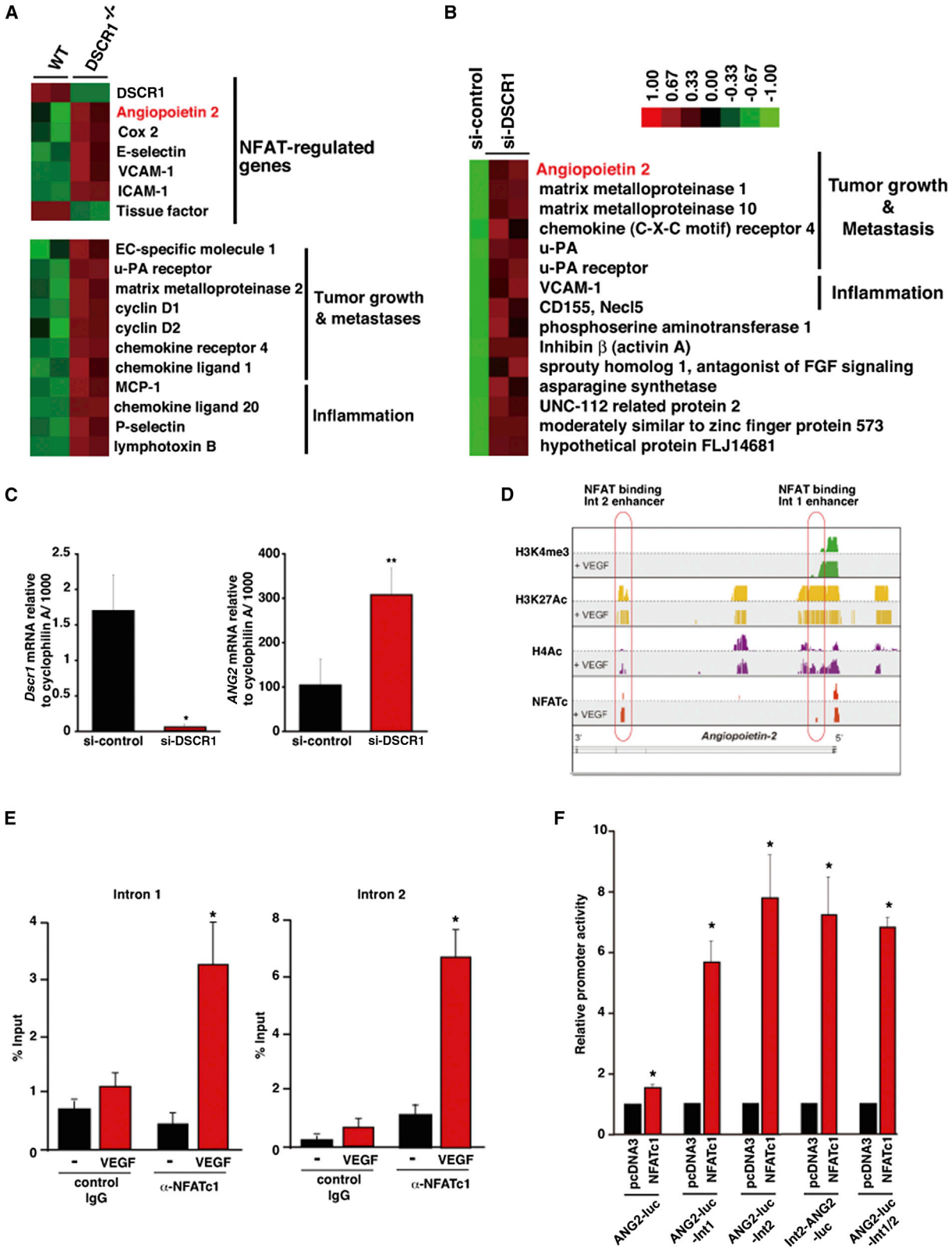

(legend on next page)

tumor xenografts (Figure 5B) due to high VEGF production by both LLC and B16-F10 tumor cells. Next, VEGFR2 activation was assessed by phospho-VEGFR2 immunofluorescence in primary tumors and lungs of WT and *Dscr1*$^{-/-}$ mice. While there was no detectable difference in VEGFR2 activation in primary tumors, there was significant phospho-VEGFR2 immunostaining in the lungs of *Dscr1*$^{-/-}$ mice, but not in WT mice (Figure 5C). We further examined VEGFR2 activation in the lung, liver, and kidney after VEGF administration and found the highest level of phospho-VEGFR2 in lung lysates (Figure 5D). This increased VEGFR2 activation in the lung may be a consequence of increased sensitivity to VEGF as compared to other organ sites. These data suggest that preferential metastases to the lung may be due in part to the increased sensitivity of lung endothelium to VEGF. Further investigation of VEGF expression in WT and *Dscr1*$^{-/-}$ mice with B16-F10 flank tumors demonstrated increased VEGF levels in the lungs of both control and tumor bearing *Dscr1*$^{-/-}$ mice (Figure 5E) similar to our observations with LLC tumors.

We have previously published that constitutively activated calcineurin signaling as a consequence of *Dscr1* loss leads to NFAT transactivation of the proapoptotic gene *FasL* on tumor endothelium (Ryeom et al., 2008). The absence of Fas ligand in our lung endothelium microarrays and the lack of apoptosis in lung metastases lead us to investigate how calcineurin-NFAT signaling could differentially regulate target genes in endothelial cells. One difference between the vasculature of lung metastases versus xenograft tumors is significantly higher VEGF levels in the primary tumor. Thus, we examined *Ang2* and *FasL* mRNA levels by qPCR in primary mouse lung endothelial cells after the addition of a range of VEGF concentrations and found that *Ang2* mRNA was preferentially upregulated at lower VEGF expression, while *FasL* mRNA was increased at considerably higher VEGF levels (Figure 5F). Taken together, these findings support a model whereby specific calcineurin-NFAT targets can be transactivated by differential VEGF levels.

Inhibition of Lung Metastases by Overexpression of DSCR1 or Soluble TIE2

Activation of calcineurin-NFAT signaling and upregulation of ANG2 expression was observed in the vasculature of microscopic lung metastases. Thus, we investigated whether genetic inhibition of calcineurin-NFAT by endothelial overexpression of DSCR1, or sequestering ANG2 with sTIE2, would be sufficient to inhibit lung metastases. We generated transgenic mice with human *DSCR1* fused to *LacZ* driven by the TIE2 promoter for endothelial specific expression demonstrated by LacZ and PECAM1 costaining in both primary flank tumors and in the lung (Figure 6A). Quantification of human *DSCR1* mRNA by qPCR in flank tumors isolated from *Tie2-DSCR1-LacZ* transgenic mice and WT littermates shows significant expression of *hDSCR1* in tumors from transgenic mice, but not control mice (Figure 6B), further indicating endothelial-specific expression of the transgene. Inhibition of calcineurin-NFAT signaling was examined by transfecting a construct with NFAT response elements driving transcription of a luciferase reporter gene into primary lung endothelial cells isolated from *Tie2-DSCR1-LacZ* and littermate controls. After treatment of cells with VEGF, WT endothelial cells show considerable luciferase activity that was significantly inhibited in *DSCR1* transgenic endothelial cells (Figure 6C).

Next, we confirmed that endothelial-specific DSCR1 overexpression was sufficient to block primary tumor growth (Figures 6D–6F) and inhibit tumor angiogenesis as shown by decreased microvessel density (Figure 6F). To determine whether lung metastases would be inhibited in our *Tie2-DSCR1-LacZ* transgenic mice, mice were inoculated subcutaneously with B16-F10 melanoma cells and lungs were examined after 3 weeks. There was a significant decrease in the incidence of lung metastases in *DSCR1* transgenic mice (Figures 6G and 6H), indicating that endothelial overexpression of *DSCR1* is sufficient to inhibit calcineurin-NFAT signaling and block both primary tumor growth and lung metastases.

sTIE2 binds to both ANG1 and ANG2 thus we examined the therapeutic potential of sTIE2 delivery in preventing lung metastases by generating an adenovirus with the TIE2 extracellular domain fused to an immunoglobulin Fc fragment (Ad-sTIE2-Fc). Measurement of plasma sTIE2 levels after systemic delivery found significant levels of sTIE2 in the plasma up to 20 days after injection (Figure 7A). Moreover, Ad-sTIE2-Fc treatment significantly reduced ANG2 in the lungs of WT and *Dscr1*$^{-/-}$ mice and also reduced ANG1 expression in the lungs of *Dscr1*$^{-/-}$ mice (Figure 7B). To ensure hyperactivation of calcineurin-NFAT in the metastatic niche, we used *Dscr1*$^{-/-}$ mice to investigate the efficacy of Ad-sTIE2-Fc on inhibiting metastases. Pretreatment of *Dscr1*$^{-/-}$ mice with sTIE2 followed by orthotopic implantation of Renca tumor cells lead to a significant decrease in lung metastases (Figure 7C). Upon delivery of sTIE2 1 day after

Figure 3. VEGF-Mediated Calcineurin-NFAT Signaling in Early Metastases in the Lung Upregulates ANG2 Expression in the Vasculature

(A and B) Heatmap of gene expression for upregulated (red) and downregulated (green) genes after VEGF treatment of (A) primary lung endothelial cells isolated from WT or *Dscr1*$^{-/-}$ mice and (B) primary lung endothelial cells treated with small interfering RNA against *Dscr1* or control (scrambled). Color intensity is relative to the median (black).

(C) qPCR of *Dscr1* and *Ang2* expression in lung endothelial cells treated with *Dscr1* or control siRNA. Results are represented as the mean ± SD relative to cyclophilin A performed in triplicate; n = 3. *$p < 0.0001$ and **$p < 0.05$ compared to si-control.

(D) ChIP sequencing (ChIP-seq) genome browser view of the *Ang2* gene. Histone marks for H3K4me3, H3K27Ac, and H4Ac are shown in green, yellow, and purple, respectively. NFATc1 binding sites and intensity are shown in red. VEGF-responsive NFATc1 binding sites that colocalize with histone enhancer marks are outlined in red.

(E) Graphs indicate the ChIP enrichment level of with anti-NFATc1 or Isotype matched control immunoglobulin G relative to total input by ChIP-qPCR. The results are represented as the mean ± SD from three independent experiments. *$p < 0.001$ compared to NFATc1 immunoprecipitation without VEGF.

(F) Human primary lung endothelial cells were transiently transfected with the indicated ANG2-luciferase (luc) construct, and either a NFATc1 expression plasmid or vector alone (pcDNA3). Results are represented as the mean ± SD of luciferase light units (relative to pcDNA3 control) performed in triplicate; n = 3. *$p < 0.01$ compared to control (pcDNA3 alone).

See also Figure S3 and Tables S2 and S3.

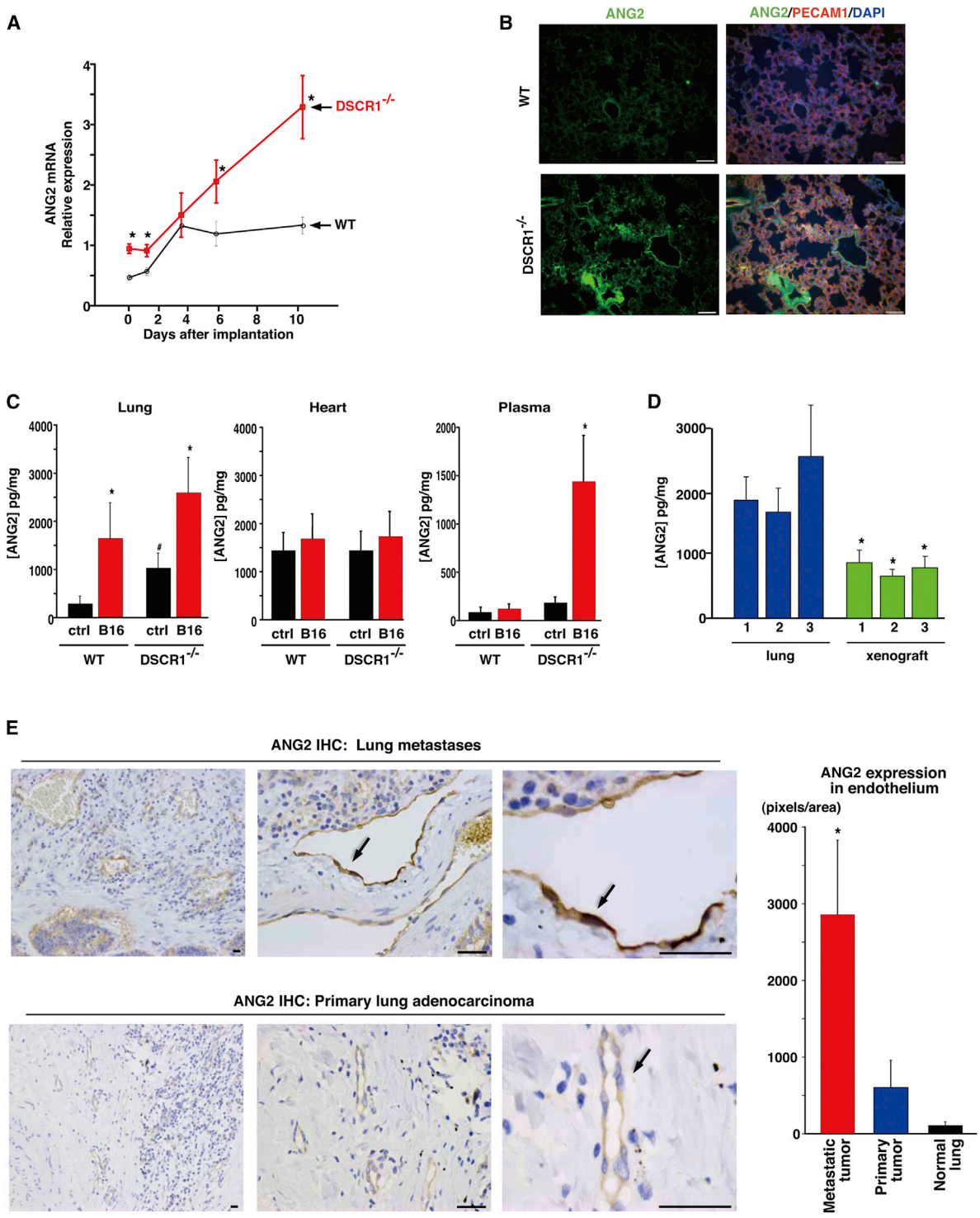

Figure 4. Increased ANG2 Expression in Lung Metastases

(A) qPCR of *Ang2* mRNA in the lungs of tumor-bearing WT or *Dscr1*$^{-/-}$ mice at the indicated days after tumor cell injection. Data are represented as the mean ± SEM relative to *β-actin* mRNA; n = 4. *p < 0.05 compared to WT at each time point.

(B) Representative immunofluorescence images of ANG2 (green) and PECAM1 (red) staining of lungs harvested from WT or *Dscr1*$^{-/-}$ mice 10 days after tumor cell inoculation. The scale bar represents 50 μm; n = 4.

(C) ANG2 levels were quantified by ELISA in lung and heart extracts and in the plasma of WT or *Dscr1*$^{-/-}$ mice with and without tumors. Data are represented as mean ± SEM; n = 10. *p < 0.05 compared to controls.

(legend continued on next page)

tail vein inoculation of B16-F10 melanoma cells, we continued to observe a significant decrease in lung lesions (Figure 7D). Microarray analysis of lungs harvested from *Dscr1*$^{-/-}$ tumor-bearing mice after sTIE2 treatment revealed significant downregulation of not only *Ang2* but also a number of genes that indicate endothelial activation such as *Vcam1* and *E-selectin* (Figures 7E and 7F). These data suggest that targeting either the calcineurin pathway or ANG2 is sufficient to suppress activation of the lung endothelium in early metastatic lesions, offering targets in the treatment of lung metastases.

DISCUSSION

Metastasis is a multistep process and is responsible for most cancer deaths. While much investigation has been devoted to understanding how tumor cells invade and extravasate from the primary site (Valastyan and Weinberg, 2011), less is understood about regulation of the metastatic site. Indeed, few studies have investigated angiogenesis regulation in the metastatic niche. Here, we examined calcineurin-NFAT signaling in lung endothelium of early metastatic lesions and found that its activation promotes metastases due to increased expression of Angiopoietin-2 (ANG2), a newly identified NFAT target. We identified ANG2 upregulation as a link between increased VEGF in the lung and increased angiogenesis in the metastatic niche promoting lung metastases. Finally, we demonstrate that inhibition of ANG2 expression by DSCR1 overexpression or by adenoviral delivery of soluble TIE2 (sTIE2) is sufficient to suppress activation of the lung endothelium in early metastatic lesions, offering targets in the treatment of lung metastases. Our data suggest that increased VEGF in the lung as a consequence of primary tumor growth activates the calcineurin-NFAT pathway upregulating ANG2 in lung endothelium, promoting angiogenesis and metastatic growth.

VEGF is the best-characterized endothelial cell mitogen with drugs targeting VEGF or its receptors to block tumor angiogenesis currently in clinical use (Wu and Staton, 2012). However, little is known about the intracellular signaling pathways that mediate VEGF effects in endothelial cells. We and others have identified the calcium-responsive calcineurin-NFAT pathway as a key intracellular regulator of VEGF in endothelial cells. VEGF ligation to VEGF receptors on endothelial cells leads to increased intracellular calcium levels and subsequent calcineurin activation. Its downregulation is modulated in part by its endogenous inhibitor, the *Dscr1* gene (Minami et al., 2004).

DSCR1 is transactivated in a calcineurin-NFAT-dependent manner and functions in a classic negative feedback loop, directly blocking calcineurin phosphatase function. Genetic deletion of *Dscr1* in a transgenic mouse model leads to hyperactivation of calcineurin-NFAT signaling (Minami et al., 2009; Ryeom et al., 2008). Although primary tumor growth was inhibited in these mice due to suppression of tumor angiogenesis, here we show a significant increase in lung metastases. To investigate the role of calcineurin-NFAT in promoting lung metastases, we generated a LacZ reporter mouse driven by the native *Dscr1* promoter as an indication of calcineurin-NFAT signaling. Inoculation of LLC in the flanks of these mice revealed calcineurin activation in lung, but not other organ endothelium, prior to the arrival of tumor cells that preferentially metastasize to the lung. Similarly, tail vein injection of tumor cells led to activation of lung endothelium prior to the detection of tumor cells in the lung. These findings support a model whereby calcineurin-NFAT activation in the vasculature of early metastatic lesions may play an important role promoting tumor cell seeding and expansion at the metastatic site.

In tumor-bearing *Dscr1*$^{-/-}$ mice, calcineurin is hyperactivated and leads to upregulation of the calcineurin-NFAT-dependent target *Ang2* in lung endothelium. In the presence of VEGF, ANG2 promotes angiogenesis by displacing ANG1 binding to the shared Angiopoietin receptor, TIE2, disrupting vessel quiescence (Saharinen and Alitalo, 2011). Although inflammatory mediators and angiogenic factors have been shown to activate ANG2 release, the molecular mechanisms regulating ANG2 expression have not yet been described. Here, we show that the calcineurin-NFAT pathway directly transactivates *Ang2* in endothelial cells in the metastatic niche. Indeed, our data show specific upregulation of ANG2 in early metastatic lesions in the lung, prior to the arrival of tumor cells that preferentially metastasize to the lung. With recent studies demonstrating an important role for calcineurin-NFAT in the innate immune system (Fric et al., 2012), it is likely that increased calcineurin-NFAT signaling in innate immune cells contribute to metastatic progression. For example, NFAT has been shown to regulate inflammatory gene expression in macrophages (Elloumi, et al., 2012), and with polarized macrophages known to promote metastasis, upregulated calcineurin-NFAT activation in these cells could play a role in the increased metastases observed in *Dscr1*$^{-/-}$ mice. However, the output of increased calcineurin signaling in macrophages from *Dscr1*$^{-/-}$ mice in the context of macrophage polarization and metastases has not yet been investigated.

While calcineurin-NFAT signaling is activated by increased intracellular calcium levels, it is clear that calcineurin function is not regulated in a straightforward binary manner. Variable levels of calcineurin activation lead to differential expression of NFAT-dependent target genes as evidenced in a number of systems. For example, in lymphocytes, primary activation of T cells leads to calcineurin-NFAT-dependent production of cytokines such as interleukin (IL)-2, IL-4, and interferon gamma, critical to mount an immune response. However, secondary activation of T cells transactivates Fas ligand initiating lymphocyte apoptosis.

(D) ANG2 levels were quantified in lung and tumor extracts harvested from tumor bearing *Dscr1*$^{-/-}$ mice. Xenografted tumors ranged from (1) ~500 mm^3 to (2) ~1,200 mm^3 to (3) ~1,500 mm^3. Data are represented as mean ± SEM; n = 3. *p < 0.01 compared to ANG2 levels in the lungs.

(E) Representative images of tumor sections from patients. Tissues from either metastatic lung lesions (upper) or primary lung adenocarcinoma (lower) were immunostained with anti-ANG2. Arrow indicates ANG2 expression in endothelial cells. The scale bar represents 50 μm. Quantification of ANG2 expression in the endothelium from metastatic lung tumors, primary lung tumors, and normal lung tissue is shown on the right. Data are represented as mean ± SEM of each section from six patients with metastatic lung tumors and 7 patients with primary lung adenocarcinoma.

See also Figures S4 and S5 and Table S4.

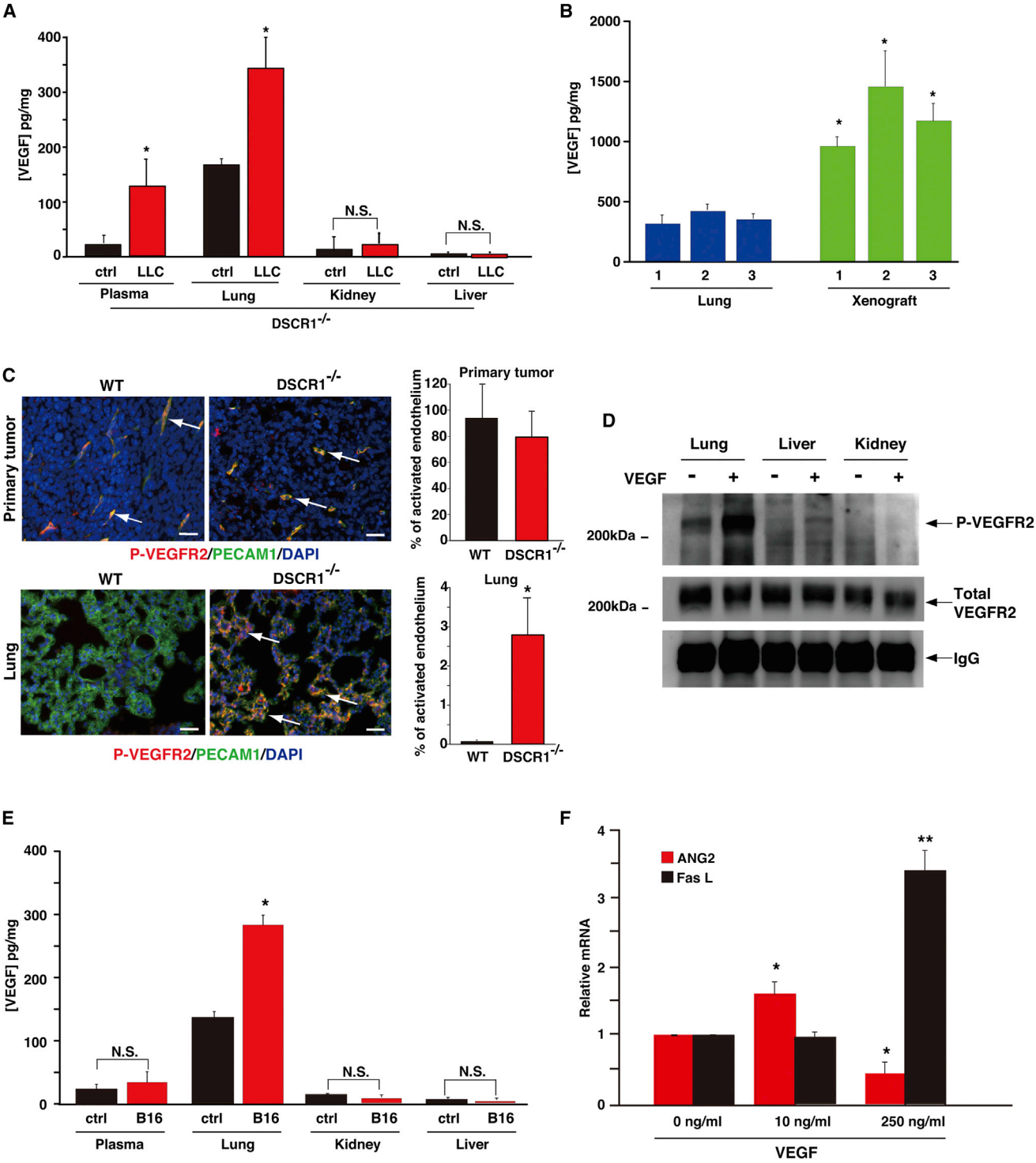

Figure 5. Increased VEGF Levels in the Lungs of Tumor-Bearing Mice

(A) VEGF levels were quantified by ELISA in the plasma, lung, kidney, or liver lysates from *Dscr1*$^{-/-}$ mice with and without LLC tumors. *$p < 0.01$ compared to each control; n = 10. NS, nonsignificant.

(B) VEGF levels were quantified in lungs and flank tumor extracts harvested from LLC tumor-bearing *Dscr1*$^{-/-}$ mice. Xenografted tumors ranged from (1) ~500 mm^3 to (2) ~1,200 mm^3 to (3) ~1,500 mm^3. Data are represented as mean ± SEM. *$p < 0.01$ compared to VEGF levels in the lungs; n = 3.

(C) Representative images of sections from LLC flank tumors (~200 mm^3) or lungs harvested from WT or *Dscr1*$^{-/-}$ mice and immunostained with antibodies against phospho-VEGFR2 (red) and PECAM1 (green). Arrows indicate costaining of phospho-VEGFR2 and PECAM1. Percentage of activated endothelium in

(legend continued on next page)

Thus, the output of calcineurin-NFAT signaling in lymphocytes is influenced by the nature of T cell activation (Ryeom et al., 2003). Similarly, we have shown in this work and previously published studies that during tumor growth, high levels of VEGF in the primary tumor microenvironment lead to upregulation of Fas ligand in endothelial cells and subsequent endothelial cell apoptosis (Ryeom et al., 2008). Conversely, more moderate levels of VEGF in the lung activate ANG2 expression in the lung endothelium, thus triggering endothelial cell activation in the lung prior to the detection of tumor cells. Further studies are needed to determine the mechanism by which VEGF levels are regulated in different organ environments during tumor growth, although it is likely that immune cell infiltration is a source of VEGF in the lungs. How varying doses of VEGF can differentially regulate calcineurin-NFAT targets also remains to be investigated, as does determining whether increasing VEGF levels control the amplitude or the duration of calcineurin signaling. It is possible that activation of specific calcineurin-NFAT targets could involve unique NFAT binding partners, downregulation of inhibitors, or different degrees of occupancy by NFAT complexes on target genes.

To determine whether the calcineurin-NFAT-ANG2 signaling axis was necessary for the establishment or progression of lung metastases, we inhibited this pathway both genetically with transgenic endothelial cell overexpression of the endogenous calcineurin inhibitor DSCR1 and by adenoviral delivery of the extracellular domain of the ANG2 receptor, soluble TIE2 (sTIE2). In both of these scenarios, lung metastases were significantly inhibited using two different transplanted tumor models that metastasize to the lung. Thus, these data implicate the requirement for calcineurin-NFAT-ANG2 signaling in the vasculature of the target organ to promote tumor metastases. Importantly, the clinical relevance of these observations is supported by our examination of both primary colon tumors and lung metastases resected from patients. Immunohistochemical studies of six patients demonstrate increased ANG2 expression specifically in the endothelium of lung metastases, but not in the vasculature of primary colon tumors, lending further confirmation of our model whereby ANG2 expression in the lung endothelium promotes metastasis to this organ.

With several antiangiogenic therapies targeting ANG2 currently being developed, understanding the mechanisms underlying ANG2 regulation in the metastatic niche are important and timely (Gerald et al., 2013). Collectively, our data implicate moderate levels of VEGF in the lungs as a key factor in regulating the calcineurin-NFAT-ANG2 pathway in lung endothelium prior to the arrival of tumor cells. Our studies indicate that activation of this pathway is necessary for lung metastases and suggest that activation of the calcineurin pathway could represent a general response of the tumor microenvironment to support the expansion of micrometastases in target organs.

EXPERIMENTAL PROCEDURES

Tumor Models and Treatment Studies

WT C57BL/6j and Balb/c mice were purchased from Clea Japan. *Dscr1*$^{-/-}$ mice on C57BL/6j and Balb/c backgrounds have been previously described (Ryeom et al., 2003). All animal care and experimental protocols were performed with the approval of the International Animal Care and Use Committee of the University of Tokyo.

For lung colonization, B16-F10 (5×10^5 cells in 100 μl PBS) cells were injected i.v. into 6-week-old WT or *Dscr1*$^{-/-}$ mice. For our tumor models, a suspension of LLC cells (2×10^6 cells per 100 μl PBS) was subcutaneously implanted into the flank region of 6-week-old WT or *Dscr1*$^{-/-}$ mice. For our orthotopic renal cell carcinoma implantation model, a suspension of Renca cells (5×10^5 cells per 50 μl Matrigel) was injected into the subcapsular space of the left kidney of WT or *Dscr1*$^{-/-}$ mice.

For CsA treatment, mice were injected with 1 mg/kg CsA or vehicle (olive oil) intraperitoneally (i.p.) every other day. For the endotoxemia model, mice were injected i.p. with normal saline (control) or LPS (16 mg/kg) from *E. coli* serotype 0111:B4 (Sigma-Aldrich). To administer adenovirus, $5 \geq 10^9$ plaque-forming units of either Ad-sTIE2-Fc or Ad-control-Fc were injected i.v.

Generation of TIE2-DSCR1-1-IRES-LacZ Transgenic Mice

The mouse *Tie2* promoter expression cassette containing 1,760 bp 5′-flanking region, exon 1 (318bp), and the core intronic enhancer (300 bp) was used for endothelial cell expression (Minami et al., 2003). The human *DSCR1* short isoform cDNA and bacterial β-galactosidase gene were subcloned into pIRES2 (Clontech) and then inserted into a *Tie2* expression cassette. The transgene was linearized by SalI and injected into mouse embryos by the transgenic facility (Tsukuba University, Japan). Mice were genotyped by Southern blotting. Three independent transgenic lines were generated and crossed onto a C57BL/6j background.

Cell Culture

Human lung primary endothelial cells were purchased and cultured in EGM-2 MV complete medium (Lonza). Isolation and culture of primary mouse endothelial cells from lung and liver were done using Miltenyi magnetic beads conjugated to anti-FITC monoclonal antibody selecting for endothelial cells after incubation with CD31-FITC and then reselected after incubation with FITC-Lectin as previously described in detail (Ryeom et al., 2008). B16-F10 cells (ATCC CRL-6475) and LLC (ATCC CRL-1642) were cultured in Dulbecco's modified Eagle's medium supplemented with 10% heat-inactivated fetal bovine serum (FBS). Renca cells (ATCC CCL-2947) were grown in RPMI 1640 medium plus 10% FBS. 3LLC (Hiratsuka et al., 2008) were grown and passaged in Balb/c nude mice.

Soluble TIE2 Adenovirus Construction

Amino acids 1–743 corresponding to exons 1–8, of mouse TIE2 (NCBI: BC050824) was amplified by PCR from mouse lung RNA and ligated to the human immunoglobulin Fc fragment. This mTIE2-Fc DNA fragment was subcloned into pENTR4 (Invitrogen) and cloned into an adenoviral vector with recombinase (Invitrogen). pAd-sTIE2-Fc was transfected into HEK293 cells for adenoviral packaging. Adenovirus titer was quantified with Adeno-X rapid titer kit (Clontech) following the manufacturer's instructions.

primary tumors and lungs was quantified as the ratio of phospho-VEGFR2 to PECAM1 positive signals. Data are represented as mean ± SD. $p < 0.0001$ compared to WT; n = 4.

(D) Western blot of phospho-VEGFR2 and total VEGFR2 expression in lung, liver, and kidney tissue harvested 10 min after treatment of WT mice with VEGF (500 mg/kg, i.v.) or control saline. The data are representative of three independent experiments.

(E) VEGF levels were quantified by ELISA in the plasma, lung, kidney, or liver tissue lysates from WT mice with and without B16-F10 tumors. *$p < 0.01$ compared to each control; n = 10.

(F) qPCR of *Ang2 and FasL* mRNA in primary lung endothelial cells after VEGF treatment at the indicated concentrations for 8 hr. Data are represented as the mean ± SD relative to *β-actin* mRNA; n = 3. *$p < 0.05$ compared to untreated.

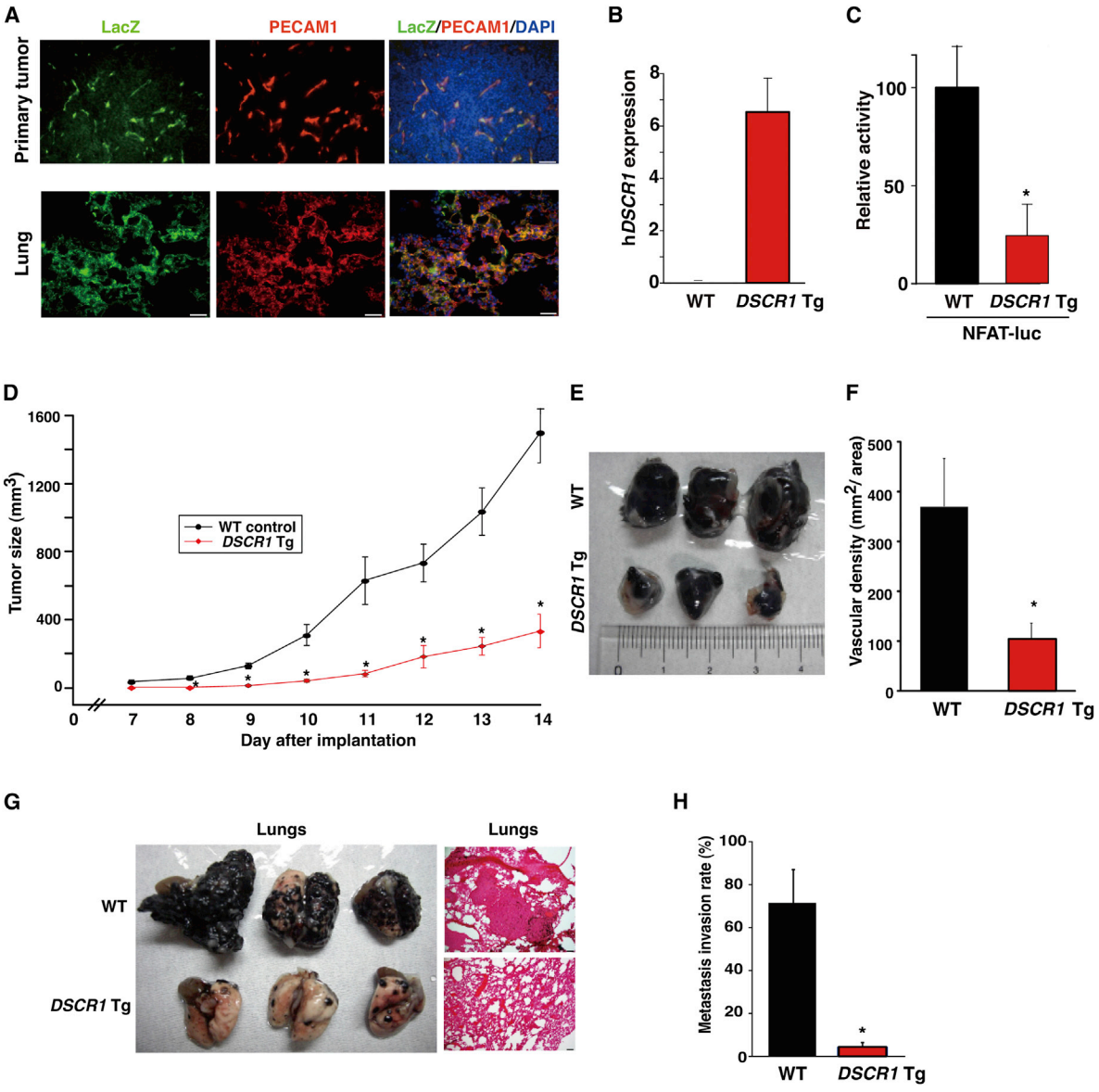

Figure 6. Endothelial-Specific Expression of DSCR1 Blocks Tumor Growth and Tumor Metastases to the Lung

(A) Representative immunofluorescence images of *lacZ* (green) and PECAM1 (red) staining of primary tumors and lungs harvested from *Tie2-h DSCR1-lacZ* transgenic (Tg) mice; n = 8.

(B) Real-time qPCR expression of h *DSCR1* mRNA in B16-F10 xenograft tumors from WT and *DSCR1* Tg mice. Results are represented as the mean ± SEM expression levels relative to *β-actin* mRNA, performed in triplicate; n = 3. *p < 0.01 compared to WT controls.

(C) Luciferase activity driven by NFAT response elements in lung endothelial cells from WT and *DSCR1* Tg mice. Results are shown as the mean ± SD of luciferase activity relative to WT performed in triplicate; n = 5. *p < 0.01 compared to luciferase activity in lung endothelial cells from WT mice.

(D) Tumor volume of B16-F10 cells was measured on the indicated days after s.c. inoculation into the flanks of WT or *DSCR1* Tg mice (n = 8).

(E) Representative images of tumor xenografts 14 days after B16-F10 inoculation from WT and *DSCR1* Tg mice; n = 8.

(F) Vascular density was quantified by PECAM1 immunostaining of sections of B16-F10 tumors harvested from WT and *DSCR1* Tg mice. Data are expressed as mean ± SD; n = 8. *p < 0.05 compared to WT.

(G) Representative images of lungs harvested from WT and *DSCR1* Tg mice 20 days after inoculation with B16-F10 cells (i.v.). H&E staining of lung sections is shown on the right. The scale bar represents 50 mm. n = 10.

(H) B16-F10 melanoma metastasis invasion rate was quantified by the percentage of metastatic tumor area relative to total lung area. *p < 0.001 compared to WT; n = 10.

See also Table S3.

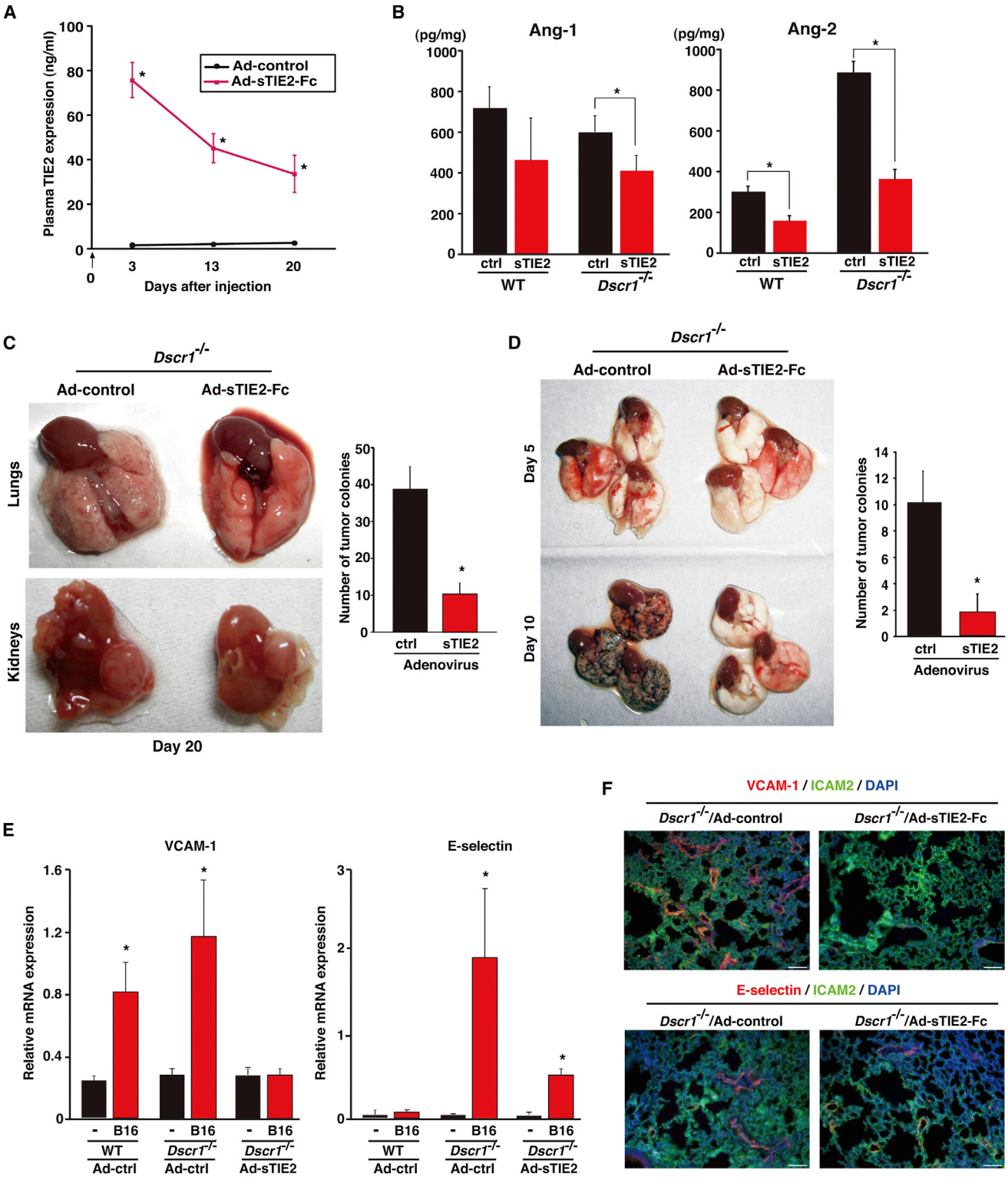

Figure 7. Adenoviral Delivery of Soluble TIE2 Decreases ANG2 Expression and Inhibits Lung Metastases

(A) Plasma sTIE2 levels were measured on the indicated days by ELISA after i.v. delivery of control (Ad-control) or adenoviral-sTIE2-Fc (Ad-sTIE2-Fc). Results are represented as the mean ± SEM; n = 8. *p < 0.001 compared to controls at each day.

(B) ANG1 and ANG2 expression were quantified by ELISA in lungs harvested from WT or *Dscr1*$^{-/-}$ mice after i.v. delivery of Ad-control or Ad-sTIE2-Fc for 4 days. Results are represented as the mean ± SEM (n = 6). *p < 0.01.

(legend continued on next page)

ANG2 Promoter Constructs

The human ANG2 promoter was cloned from the BAC clone RP11-1065H2. Promoter region (−580 to +330) was amplified by PCR and subcloned into pGL4.10 (Promega). Intron 1 and intron 2 of ANG2 was amplified by PCR and subcloned into the pGL4.10. Consensus NFAT binding sites are indicated in bold in Table S2, with point mutations (GGAA to GACT) generated using the QuikChange XL site-directed mutagenesis kit (Stratagene). Promoter sequences are shown in Table S2.

Immunohistochemistry

Mice were perfused with 2% paraformaldehyde in PBS. Tissues were harvested and fixed with 2% paraformaldehyde then immersed in 30% sucrose for 20 hr at 4°C. Cyrosectioned slides were treated with acetone for 10 min, blocked with protein blocker (Dako), and incubated with first antibody for 20 hr at 4°C. Slides were washed and incubated with an Alexa Fluor-labeled secondary antibody (Invitrogen) for 1 hr, washed in PBS, mounted in ProLong Gold anti-fade reagent with DAPI (Invitrogen), and examined by fluorescent microscopy. Antibodies against PECAM1, VCAM1, E-selectin, ICAM2, and TIE2 were obtained from BD PharMingen. Antibodies against LacZ and ANG2 were from MBL and Abcam, respectively. Anti-ANG1 was from Millipore. Anti-DSCR1 was described previously (Minami et al., 2006).

DNA Microarray

Endothelial cells or whole-lung RNAs were harvested and purified with TRIzol (Invitrogen). Preparation of complementary RNA and hybridization of probe arrays were performed according to the manufacturer's instructions (Affymetrix) with detailed protocols provided in the Extended Experimental Procedures. Annotation of the probe numbers and targeted sequences are shown on the Affymetrix web page.

ChIP-Seq Analysis

All protocols for Illumina/Solexa sequence preparation, sequencing, and quality control were according to Illumina with some modifications as previously described (Kanki et al., 2011). Detailed protocols are provided in the Extended Experimental Procedures.

VEGFR2 Activation

Murine recombinant VEGF (Peprotec) was administrated (i.v.) to WT C57BL/6j mice. Ten minutes later, lung, liver, and kidney tissue were harvested and lysed with RIPA buffer (Cell Signaling). Protein concentrations from whole-tissue extracts were quantified and 12 μg of each tissue was immunoprecipitated with anti-VEGFR2 (Flk-1) antibody (Cell Signaling). Immunoprecipitated samples were separated by SDS-PAGE and probed with a phospho-specific VEGFR2 antibody (Cell Signaling). The membrane was stripped and reprobed with total VEGFR2 antibody.

VEGF, ANG1, ANG2, and Soluble TIE2 Levels

Blood or tissue homogenates were collected from the indicated mice and centrifuged. Plasma or tissue eluents were harvested and each sample was diluted to 5- to 200-fold. VEGF and soluble TIE2 levels were measured using Quantikine ELISA kits (R&D Systems). ANG1 and ANG2 level were measured by an ELISA kit (UCSN Life Science).

Statistics

Data are presented as mean ± SD or SEM as indicated. p values were calculated using a two-tailed unpaired Student's t test. The Wilcoxon log-rank test was used for mouse survival studies. Statistical tests and graphing were done with KaleidaGraph (Synergy Software). A p value less than 0.05 was considered significant.

For further details, please refer to the Extended Experimental Procedures and Tables S3 and S4.

ACCESSION NUMBERS

The NCBI accession number for the data reported in this paper is GSE48841.

SUPPLEMENTAL INFORMATION

Supplemental Information includes Extended Experimental Procedures, five figures, and four tables and can be found with this article online at http://dx.doi.org/10.1016/j.celrep.2013.07.021.

ACKNOWLEDGMENTS

We would like to thank S. Hiratsuka and Y. Maru (Tokyo Women's Medical University) for providing 3LLC and M. Shibuya (the University of Tokyo) for advice and the transgenic facility in Tsukuba University (Japan) for generating the *Dscr1* Tg mice. We are grateful to the members of the Minami and Ryeom labs for their input. This work was supported by Leading-Edge Research Promotion fund from the Japan Society (LS038, T.M.), The Garrett B. Smith Foundation (S.R.), the TED-driven Foundation (S.R.), and grants P01 CA045548 (S.R.) and R01 CA118374 (S.R.). T.M. and S.R. designed, supervised, and conducted experiments and data analyses and wrote the manuscript. J-i.S. and T.O. performed transgenic mice analyses. S.J. and M.N. performed immunohistochemical stainings with human clinical studies. M.M. and K. S. performed experiments and data analyses. Y.O. and T.K. provided advice throughout the project.

Received: May 8, 2013
Revised: June 25, 2013
Accepted: July 17, 2013
Published: August 15, 2013

REFERENCES

Baek, K.H., Zaslavsky, A., Lynch, R.C., Britt, C., Okada, Y., Siarey, R.J., Lensch, M.W., Park, I.H., Yoon, S.S., Minami, T., et al. (2009). Down's syndrome suppression of tumour growth and the role of the calcineurin inhibitor DSCR1. Nature *459*, 1126–1130.

Bergers, G., and Hanahan, D. (2008). Modes of resistance to anti-angiogenic therapy. Nat. Rev. Cancer *8*, 592–603.

De Palma, M., Venneri, M.A., Roca, C., and Naldini, L. (2003). Targeting exogenous genes to tumor angiogenesis by transplantation of genetically modified hematopoietic stem cells. Nat. Med. *9*, 789–795.

(C) Representative images of lungs and kidneys harvested from *Dscr1*$^{-/-}$ mice after treatment of mice with Ad-control or Ad-sTIE2-Fc prior to orthotopic injections of Renca cells in the kidney. Organs were harvested 20 days after tumor cell injection. The number of tumor colonies per hpf in the lungs is shown on the right with results represented as the mean ± SD. *p < 0.0001 compared to Ad-control; n = 6.

(D) Representative images of lungs harvested from *Dscr1*$^{-/-}$ mice at the indicated days after B16-F10 i.v. injection. Ad-control or Ad-sTIE2-Fc were injected 24 hr after tumor cell inoculation. The number of tumor colonies are shown on the right with results presented as the mean ± SD. *p < 0.01 compared to Ad-control; n = 6.

(E) qPCR of *Vcam-1* and *E-selectin* mRNA in lungs harvested from either WT or *Dscr1*$^{-/-}$ mice with and without B16-F10 flank tumors treated with either Ad-control or Ad-sTIE2-Fc. Results are represented as the mean ± SD expression levels relative to *β-actin* mRNA, performed in triplicate; n = 3. *p < 0.01 compared to non-tumor-bearing mice.

(F) Representative images of lung sections harvested from *Dscr1*$^{-/-}$ mice after i.v. injection of B16-F10 melanoma cells and treatment with either Ad-control or Ad-sTIE2. Sections were immunostained with antibodies to VCAM-1 (red), ICAM2 (green), and DAPI (blue) (upper row) or E-selectin (red), ICAM2 (green), and DAPI (blue) (lower row). The scale bar represents 50 μm.

De Palma, M., Venneri, M.A., Galli, R., Sergi Sergi, L., Politi, L.S., Sampaolesi, M., and Naldini, L. (2005). Tie2 identifies a hematopoietic lineage of proangiogenic monocytes required for tumor vessel formation and a mesenchymal population of pericyte progenitors. Cancer Cell *8*, 211–226.

Eklund, L., and Saharinen, P. (2013). Angiopoietin signaling in the vasculature. Exp. Cell Res. *319*, 1271–1280.

Elloumi, H.Z., Maharshak, N., Rao, K.N., Kobayashi, T., Ryu, H.S., Mühlbauer, M., Li, F., Jobin, C., and Plevy, S.E. (2012). A cell permeable peptide inhibitor of NFAT inhibits macrophage cytokine expression and ameliorates experimental colitis. PLoS ONE *7*, e34172.

Erler, J.T., Bennewith, K.L., Cox, T.R., Lang, G., Bird, D., Koong, A., Le, Q.T., and Giaccia, A.J. (2009). Hypoxia-induced lysyl oxidase is a critical mediator of bone marrow cell recruitment to form the premetastatic niche. Cancer Cell *15*, 35–44.

Fric, J., Zelante, T., Wong, A.Y., Mertes, A., Yu, H.B., and Ricciardi-Castagnoli, P. (2012). NFAT control of innate immunity. Blood *120*, 1380–1389.

Gerald, D., Chintharlapalli, S., Augustin, H.G., and Benjamin, L.E. (2013). Angiopoietin-2: an attractive target for improved antiangiogenic tumor therapy. Cancer Res. *73*, 1649–1657.

Hegen, A., Koidl, S., Weindel, K., Marmé, D., Augustin, H.G., and Fiedler, U. (2004). Expression of angiopoietin-2 in endothelial cells is controlled by positive and negative regulatory promoter elements. Arterioscler. Thromb. Vasc. Biol. *24*, 1803–1809.

Hesser, B.A., Liang, X.H., Camenisch, G., Yang, S., Lewin, D.A., Scheller, R., Ferrara, N., and Gerber, H.P. (2004). Down syndrome critical region protein 1 (DSCR1), a novel VEGF target gene that regulates expression of inflammatory markers on activated endothelial cells. Blood *104*, 149–158.

Hiratsuka, S., Watanabe, A., Sakurai, Y., Akashi-Takamura, S., Ishibashi, S., Miyake, K., Shibuya, M., Akira, S., Aburatani, H., and Maru, Y. (2008). The S100A8-serum amyloid A3-TLR4 paracrine cascade establishes a premetastatic phase. Nat. Cell Biol. *10*, 1349–1355.

Holash, J., Maisonpierre, P.C., Compton, D., Boland, P., Alexander, C.R., Zagzag, D., Yancopoulos, G.D., and Wiegand, S.J. (1999). Vessel cooption, regression, and growth in tumors mediated by angiopoietins and VEGF. Science *284*, 1994–1998.

Kanki, Y., Kohro, T., Jiang, S., Tsutsumi, S., Mimura, I., Suehiro, J., Wada, Y., Ohta, Y., Ihara, S., Iwanari, H., et al. (2011). Epigenetically coordinated GATA2 binding is necessary for endothelium-specific endomucin expression. EMBO J. *30*, 2582–2595.

Kaplan, R.N., Riba, R.D., Zacharoulis, S., Bramley, A.H., Vincent, L., Costa, C., MacDonald, D.D., Jin, D.K., Shido, K., Kerns, S.A., et al. (2005). VEGFR1-positive haematopoietic bone marrow progenitors initiate the pre-metastatic niche. Nature *438*, 820–827.

Minami, T., Kuivenhoven, J.A., Evans, V., Kodama, T., Rosenberg, R.D., and Aird, W.C. (2003). Ets motifs are necessary for endothelial cell-specific expression of a 723-bp Tie-2 promoter/enhancer in Hprt targeted transgenic mice. Arterioscler. Thromb. Vasc. Biol. *23*, 2041–2047.

Minami, T., Horiuchi, K., Miura, M., Abid, M.R., Takabe, W., Noguchi, N., Kohro, T., Ge, X., Aburatani, H., Hamakubo, T., et al. (2004). Vascular endothelial growth factor- and thrombin-induced termination factor, Down syndrome critical region-1, attenuates endothelial cell proliferation and angiogenesis. J. Biol. Chem. *279*, 50537–50554.

Minami, T., Miura, M., Aird, W.C., and Kodama, T. (2006). Thrombin-induced autoinhibitory factor, Down syndrome critical region-1, attenuates NFAT-dependent vascular cell adhesion molecule-1 expression and inflammation in the endothelium. J. Biol. Chem. *281*, 20503–20520.

Minami, T., Yano, K., Miura, M., Kobayashi, M., Suehiro, J., Reid, P.C., Hamakubo, T., Ryeom, S., Aird, W.C., and Kodama, T. (2009). The Down syndrome critical region gene 1 short variant promoters direct vascular bed-specific gene expression during inflammation in mice. J. Clin. Invest. *119*, 2257–2270.

Ryeom, S., Greenwald, R.J., Sharpe, A.H., and McKeon, F. (2003). The threshold pattern of calcineurin-dependent gene expression is altered by loss of the endogenous inhibitor calcipressin. Nat. Immunol. *4*, 874–881.

Ryeom, S., Baek, K.H., Rioth, M.J., Lynch, R.C., Zaslavsky, A., Birsner, A., Yoon, S.S., and McKeon, F. (2008). Targeted deletion of the calcineurin inhibitor DSCR1 suppresses tumor growth. Cancer Cell *13*, 420–431.

Saharinen, P., and Alitalo, K. (2011). The yin, the yang, and the angiopoietin-1. J. Clin. Invest. *121*, 2157–2159.

Saharinen, P., Eklund, L., Pulkki, K., Bono, P., and Alitalo, K. (2011). VEGF and angiopoietin signaling in tumor angiogenesis and metastasis. Trends Mol. Med. *17*, 347–362.

Simon, M.P., Tournaire, R., and Pouyssegur, J. (2008). The angiopoietin-2 gene of endothelial cells is up-regulated in hypoxia by a HIF binding site located in its first intron and by the central factors GATA-2 and Ets-1. J. Cell. Physiol. *217*, 809–818.

Valastyan, S., and Weinberg, R.A. (2011). Tumor metastasis: molecular insights and evolving paradigms. Cell *147*, 275–292.

Welford, A.F., Biziato, D., Coffelt, S.B., Nucera, S., Fisher, M., Pucci, F., Di Serio, C., Naldini, L., De Palma, M., Tozer, G.M., and Lewis, C.E. (2011). TIE2-expressing macrophages limit the therapeutic efficacy of the vascular-disrupting agent combretastatin A4 phosphate in mice. J. Clin. Invest. *121*, 1969–1973.

Wu, J.M., and Staton, C.A. (2012). Anti-angiogenic drug discovery: lessons from the past and thoughts for the future. Expert Opin. Drug Discov. *7*, 723–743.